

EVIDENCE FOR JET-CLOUD INTERACTIONS IN HIGH-REDSHIFT RADIO GALAXIES

C. Solórzano-Iñarrea,^{1,2} C. N. Tadhunter,¹ and D. J. Axon³

RESUMEN

Presentamos los resultados obtenidos de un estudio, basado en espectroscopía de rendija larga, de los mecanismos de cinemática y de ionización del gas de emisión de línea para una muestra de cinco radio galaxias de corrimiento al rojo alto/intermedio. En dos de las galaxias (3C352 y 3C435A) las fuentes de radio son de la misma escala que las regiones de emisión de línea, mientras que en las otras tres (3C34, 3C265 y 3C330) las fuentes de radio son mucho más extensas que las estructuras de emisión de línea. Vemos que hay evidencia de aceleración de choque del gas de emisión de línea en las regiones extendidas de *todas* las galaxias, incluso en las fuentes de radio más grandes de nuestra muestra, en las cuales los puntos calientes de radio han pasado el gas extendido de las galaxias. Las regiones extendidas presentan cinemáticas altamente disturbadas (separación de líneas y/o componentes anchas subyacentes), que son difíciles de explicar si no se considera una fuerte interacción entre las componentes de emisión de radio y el gas ambiente. Sin embargo, el mecanismo dominante de la ionización del gas de emisión de línea sigue siendo incierto. Hemos comparado las razones entre las líneas diagnósticas en el óptico de las galaxias de nuestra muestra con modelos de fotoionización debida al núcleo de galaxia activa (NGA) y modelos de ionización de choque. No encontramos consistencia al explicar el mecanismo principal de la ionización. Esto sugiere que, si las regiones extendidas son ionizadas por choques, algunas de los suposiciones implícitas en los modelos necesitan ser reconsideradas.

ABSTRACT

We report the results obtained from a study, based on long-slit spectroscopy, of the kinematics and ionization mechanisms of the line-emitting gas for a sample of five high/intermediate-redshift radio galaxies. In two of the galaxies (3C352 and 3C435A) the radio sources are of the same scale as the emission-line regions, whereas in the other three (3C34, 3C265 and 3C330) the radio sources are extended on a larger scale than the emission-line structures. We see evidence for shock-acceleration of the emission-line gas in the extended regions of *all* the galaxies, even in the largest radio sources of our sample, in which the radio hot spots have passed the extended gas of the galaxies. The extended regions present highly disturbed kinematics (line-splitting and/or underlying broad components), which are difficult to explain if we do not consider a strong interaction between the radio-emitting components and the ambient gas. However, the dominant ionization mechanism of the line-emitting gas remains uncertain. We have compared the optical diagnostic line ratios of the galaxies in our sample with both photoionization from the active galactic nucleus (AGN) and shock-ionization models. We find a lack of consistency in explaining the main ionization mechanism. This suggests that, if the extended regions are shock-ionized, some of the assumptions implicit in the models may need to be reconsidered.

Key Words: GALAXIES: ACTIVE — GALAXIES: JETS — GALAXIES: KINEMATICS AND DYNAMICS

1. INTRODUCTION

The extended emission-line regions (EELR), which are present in most powerful radio galaxies, offer the possibility of investigating the origin of the activity and the origin of the gas itself. If we are going to use the EELR in this way, we need to understand the mechanisms involved in kinematics and ionization of the EELR in these sources. How-

ever, the nature of these mechanisms remains highly uncertain. Currently, the two most accepted models are AGN-photoionization, which is in agreement with the unified schemes (e.g., Barthel 1989), and jet-cloud interactions. At low redshifts, the properties of the EELR in most radio galaxies are consistent with AGN-photoionization, and the kinematics can be explained in terms of pure gravitational motion (Tadhunter et al. 1989). However, some nearby radio galaxies show clear evidence for strong interactions between the radio-emitting components and

¹University of Sheffield, Sheffield, UK.

²University of Leeds, Leeds, UK.

³University of Hertfordshire, Hatfield, UK.

the ambient gas (Clark et al. 1997, 1998). Features observed in these galaxies include: (a) close morphological association between radio and optical emission; (b) complex kinematics; (c) large linewidths in the extended gas; and (d) anticorrelations between linewidth and ionization state. At higher redshifts powerful radio galaxies frequently show highly collimated UV continuum and emission-line structures which are closely aligned with the radio axes (Best, Longair, Röttgering 1996). Such collimated structures are not what would be expected on the basis of the unified schemes. In addition, many high-redshift radio galaxies present highly disturbed emission-line kinematics along the radio axis, which are difficult to explain in terms of pure gravitational motions.

Recent studies at $z \simeq 1$ reveal that there is a strong evolution of the emission-line properties of powerful radio galaxies with radio size (Best et al. 2000). It is found that small radio sources are consistent with shock ionization, while the larger radio sources, in which the shock fronts have passed beyond the EELR, are consistent with AGN photoionization. In contrast, a study at $z > 2$, based on UV line ratios of a sample of radio galaxies, shows that the EELR are mainly photoionized by the central AGN (Villar-Martín, Tadhunter, Clark 1997). However, we have to be cautious when comparing the results from samples at different redshifts, given that optical observations sample different rest wavelengths as the redshift varies. Consequently, the diagnostic diagrams used to determine the ionization mechanism involve lines of different ionization as the redshift changes, and there is a danger that our sensitivity to particular ionization mechanisms varies with wavelength.

Our data cover optical rest wavelengths, thereby allowing direct comparisons to be made between low- and high- z objects. With these observations we extend the approach of combining kinematical and ionization information to the higher redshift regimes. Low- z radio galaxies with jet-cloud interactions present a UV continuum excess mainly dominated by the nebular continuum emission. In this regard, we investigate the contribution of the nebular continuum to the UV excess in the galaxies of our sample.

2. THE DATA

Our sample consists of five 3C radio galaxies with high/intermediate redshifts. The galaxies are the following: 3C34 ($z = 0.690$), 3C265 ($z = 0.811$), 3C330 ($z = 0.550$), 3C352 ($z = 0.8067$) and 3C435A ($z = 0.471$). All five objects were previously known

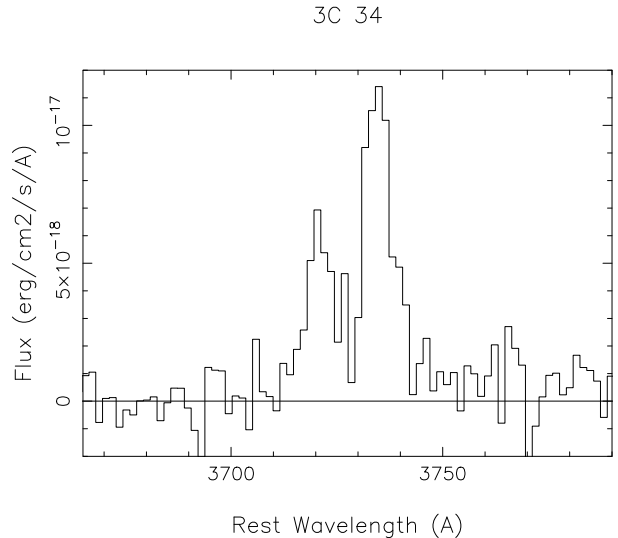


Fig. 1. Extracted spectrum of 3C34 showing the split components in the [O II] line.

as having EELR aligned along their radio axes. We also selected the sources so as to have different radio sizes relative to the corresponding host galaxies.

3. EXTREME KINEMATICS

All the sources in our sample present disturbed off-nuclear emission-line kinematics; not just those sources in which the radio and emission line structures have a similar scale, but also those with the most extended radio sources, in which the main radio emitting components have passed beyond the EELR.

Line splitting is observed in 3C34, 3C265 and 3C330. Figure 1 presents the extracted spectrum of 3C34 showing the high velocity components to the [O II] line. The variations in the velocity centroids along the radio axis of 3C34 for [O II] and [O III] are shown in Figure 2. A strong splitting ($\Delta v \sim 1000 \text{ km s}^{-1}$) in both emission lines can be observed at a radial distance of 2 to 4.5 arcsec on the west side of the nucleus. These velocity shifts are too large to be explained by gravitational motions; rather, they are most likely the result of interactions between the radio plasma and the interstellar medium. However, it is not yet clear whether direct shock acceleration associated with the radio components is sufficient to accelerate the clouds to such high velocities (Villar-Martín et al. 1999). Some entrainment of the clouds in the post-shock wind and/or in the turbulent boundary layers of the radio jets is required (see Solórzano-Iñarrea, Tadhunter, & Axon 2001 and references therein).

Further evidence for jet-cloud interactions is provided by the existence of broad kinematic compo-

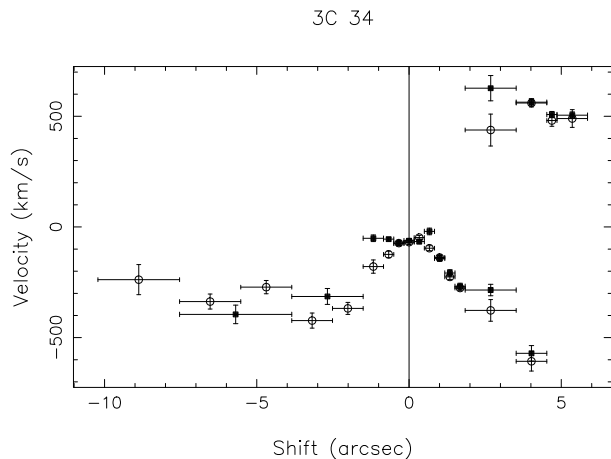


Fig. 2. Variation in the rest-frame radial velocity along the radio axis of 3C34 for [O II] (open circles) and [O III] (filled squares). West is to the right.

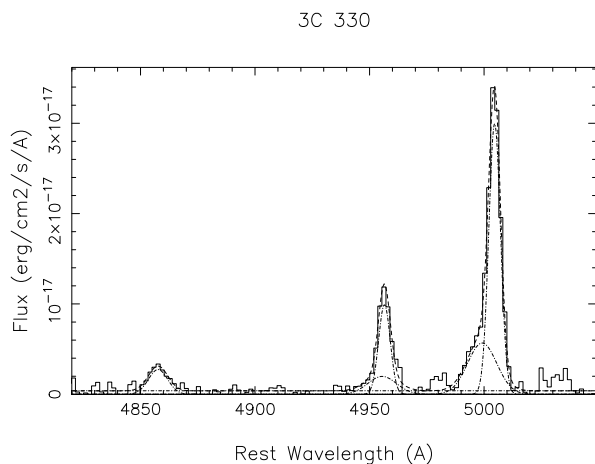


Fig. 3. $H\beta$, [O III] λ 4959 and [O III] λ 5007 emission-line profiles from the spectrum of 3C330. Two-component Gaussian fits (dot-dash-dot-dash lines) and total fit (dashed line) are also plotted.

nents in the emission lines of some of the radio galaxies. The broad component is believed to represent gas cooling behind the shock fronts and is found to be spatially associated with the radio emitting structures (Villar-Martín et al. 1999). We have detected underlying broad components (FWHM \sim 1000–1500 km s $^{-1}$) in the line profiles of four galaxies in our sample (3C265, 3C330, 3C352 and 3C435A), in addition to narrow components. Figure 3 shows the $H\beta$ and [O III] emission-line profiles from the spectrum of 3C330. The broad wing in the [O III] λ 5007 line suggests the existence of the broad component. Similar kinematically disturbed components are observed in 3C265, 3C352 and 3C435A (Solórzano-Íñarrea et al. 2001).

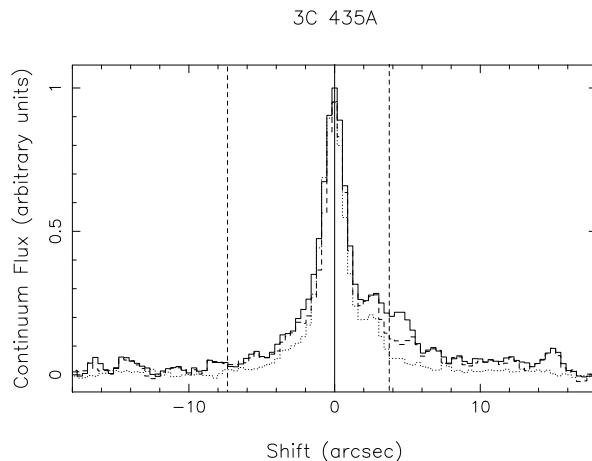


Fig. 4. Line-free continuum emission profile along the radio axis of 3C435A. The solid line shows the 2600–3700 Å profile, the dashed line shows the nebular-subtracted blue-continuum, and the dotted line shows the 5200–6000 Å profile. (NE is to the right.)

Overall, the complex kinematics observed in the EELR of the galaxies in our sample indicate that the material has been highly perturbed and accelerated by the interaction between the radio emitting components and the ambient gas. We see evidence for this shock acceleration even in those galaxies with the more extended radio sources (3C34, 3C265 and 3C330), in which the radio hot spots have passed well beyond the EELR.

4. CONTINUUM EMISSION

We have investigated the nebular continuum contribution to the UV excess in the galaxies in our sample. We find a significant nebular emission contribution to the UV continuum in all cases, with the nebular contribution ranging from \sim 10 per cent in the nuclei of 3C34 and 3C435A, to \sim 40 per cent in the extended regions of 3C330. However, following subtraction of the nebular component, a significant UV excess remains in the extended nebulae in most of the objects (Solórzano-Íñarrea et al. 2001). Figure 4 shows the spatial profile of the continuum emission along the radio axis of 3C435A. The solid line represents the UV continuum, the dashed line represents nebular-subtracted UV continuum, and the dotted line represents the red continuum (scaled to the peak of the nebular-subtracted UV profile). By comparing the nebular-subtracted UV continuum and the red continuum, it can be seen that the nebular continuum cannot account for the UV continuum excess observed on both sides of the nucleus.

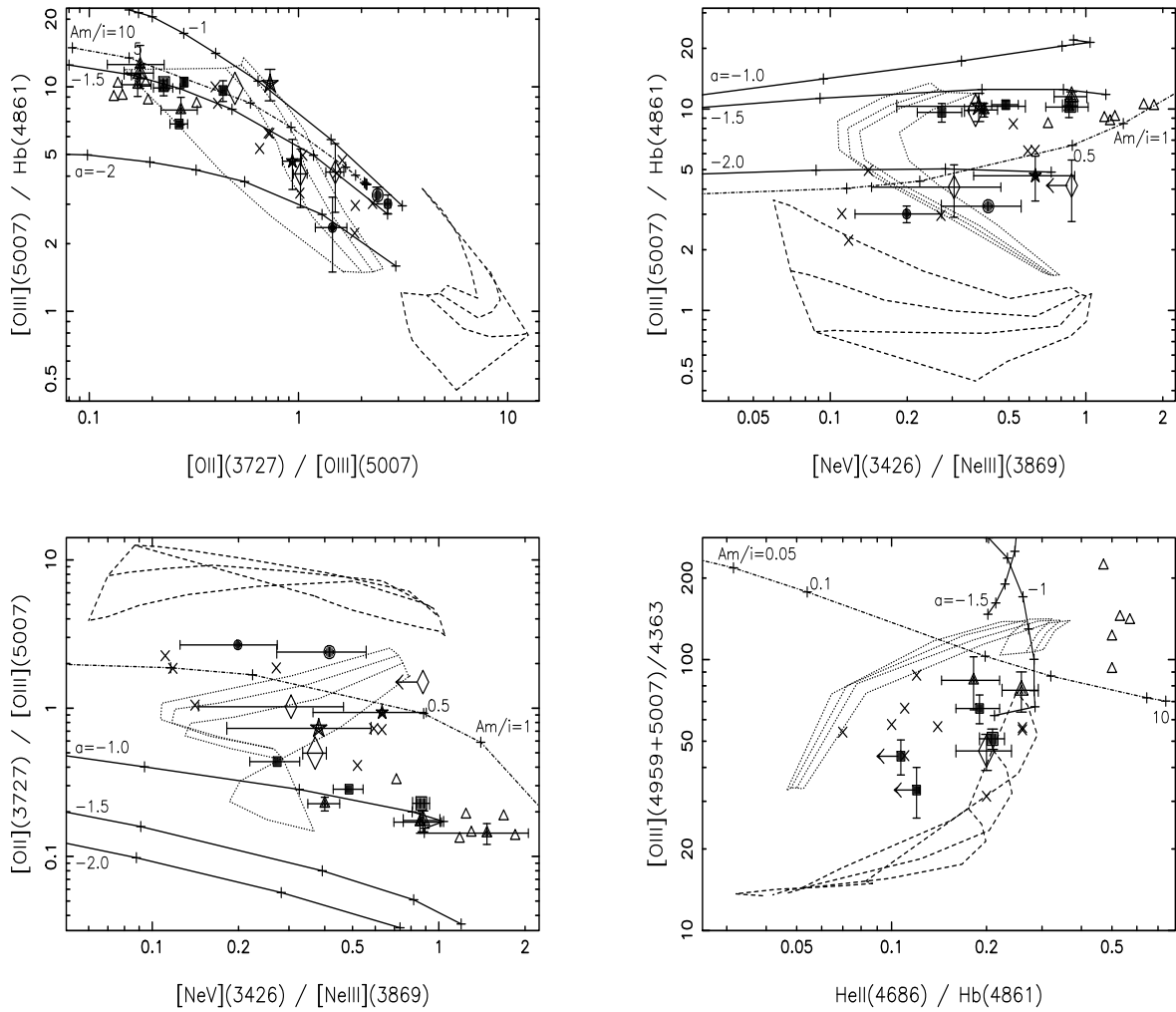


Fig. 5. Diagnostic diagrams showing the following line ratios: (a) $[\text{O III}] 5007/\text{H}\beta$ versus $[\text{O II}] 3727/[\text{O III}] 5007$; (b) $[\text{O III}] 5007/\text{H}\beta$ versus $[\text{Ne V}] 3426/[\text{Ne III}] 3869$; (c) $[\text{O II}] 3727/[\text{O III}] 5007$ versus $[\text{Ne V}] 3426/[\text{Ne III}] 3869$; and (d) $[\text{O III}] (4959 + 5007)/4363$ versus $\text{He II } 4686/\text{H}\beta$ for the four sources: 3C34 (stars), 3C265 (filled triangles); 3C330 (filled squares), 3C352 (open diamonds) and 3C435A (filled circles). Bigger symbols denote the nuclear regions and smaller ones the extended regions of the galaxies. For comparison, line ratios corresponding to the EELR of low-redshift radio galaxies are also plotted: shock-ionized (crosses) and photoionized objects (open triangles). Pluses linked by solid lines represent line ratios produced by optically-thick single-slab power-law ($F_\nu \propto \nu^\alpha$) photoionization models (using the code MAPPINGS) with spectral indices of $\alpha = -1.0, -1.5$ and -2.0 , and a sequence in the ionization parameter covering the range $5 \times 10^{-4} < U < 10^{-1}$. Pluses linked by a dot-dash-dot line indicate the predictions of the photoionization including matter-bounded clouds model from Binette et al. (1996), with the ratio $A_{M/I}$ in the range $10^{-4} \leq A_{M/I} \leq 10$. U and $A_{M/I}$ increase from right to left in (a), and from left to right in (b), (c) and (d). Predictions of pure shocks (dashed lines), and 50 per cent shocks + 50 per cent precursor models (dotted lines) from Dopita & Sutherland (1995, 1996) are also plotted, each sequence corresponding to a fixed magnetic parameter ($B/\sqrt{n} = 0, 1, 2, 4 \mu\text{G cm}^{-3/2}$) and a changing shock velocity in the range $150 \leq v_s \leq 500 \text{ km s}^{-1}$.

5. IONIZATION MECHANISM

Although there is evidence for shock-acceleration of the extended gas in the galaxies of our sample, this does not necessarily imply that the clouds are shock-ionized. To address the issue of the ionization

mechanism, we have compared the measured line ratios of the galaxies in our sample with the predictions of various ionization models, including: power-law photoionization (using the code MAPPINGS), mixed-medium photoionization (from Binette et al. 1996), pure-shock ionization and shocks including a

photoionized precursor (from Dopita & Sutherland 1995, 1996).

Figure 5 shows the resulting diagnostic diagrams, which involve the line pairs: [Ne V] λ 3426 & [Ne III] λ 3869, [O II] λ 3727 & [O III] λ 5007, $H\beta$ & [O III] λ 5007, He II(4686) & $H\beta$ and the electron temperature diagnostic line ratio [O III] (4959 + 5007)/4363. By comparing the diagnostic diagrams (a), (b) and (c), we see that pure-shock predictions (dashed lines) are inconsistent with the data, and it appears that both mixed-medium photoionization (dot-dash-dot line) and shock+precursor models (dotted lines) provide a good fit. However, in the temperature diagnostic diagram (d) the data appear to be more consistent with the pure-shock than with any of the other models.

There is a general inconsistency from diagram to diagram for individual sources, as well as for the ensemble of points for all the galaxies together. Particularly problematic is the temperature diagnostic diagram (d). If we consider this diagram, it can be seen that the [O III] (4959 + 5007)/4363 line ratios of the data are lower, and nearer to the pure-shock predictions than we would expect on the basis of the other three diagrams. This discrepancy could be explained if we consider that the post-shock clouds are destroyed by the interaction with the hot post-shock wind as they cool. By reducing the size of the post-shock cooling zone, weaker emissions in [O II] and $H\beta$ would be measured, while the [O III] emission would not be affected. Therefore, we expect to measure lower [O II]/[O III] ratios and higher [O III]/ $H\beta$ ratios than predicted by the models, but we would expect the [O III] (4959 + 5007)/4363 ratio to be unaffected. This could explain the inconsistency between the results of the temperature diagnostic diagram and diagrams (a), (b) and (c). This idea of “matter-bounded shocks” needs to be checked with more detailed modelling.

6. CONCLUSIONS

We see evidence for shock-acceleration of the gas of emission-line gas in the EELR of all the galaxies, even in the largest radio sources of our sample, in which the radio hot spots have passed the extended the galaxies. However, we do not find consistency in explaining the dominant ionization mechanism of the line-emitting gas. Our results suggest that, if the EELR are shock-ionized, some of the assumptions implicit in the models might be wrong.

This work is based on observations made at the Observatorio del Roque de los Muchachos, La Palma, Spain.

REFERENCES

- Barthel, P. D. 1989, *ApJ*, 336, 606
 Best, P. N., Longair, M. S., & Röttgering, H. J. A. 1996, *MNRAS*, 280, L9
 Best, P. N., Röttgering, H. J. A., & Longair, M. S. 2000, *MNRAS*, 311, 23
 Binette, L., Wilson, A. S., & Storchi-Bergmann, T. 1996, *A&A*, 312, 365
 Clark, N. E., Axon, D. J., Tadhunter, C. N., Robinson, A., & O’Brien, P. 1998, *ApJ*, 494, 546
 Clark, N. E., et al. 1997, *MNRAS*, 286, 558
 Dopita, M. A., & Sutherland, R. S. 1995, *ApJ*, 455, 468
 ———. 1996, *ApJS*, 102, 161
 Solórzano-Iñarrea, C., Tadhunter, C. N., & Axon, D. J. 2001, *MNRAS*, in press
 Tadhunter, C. N., Fosbury, R. A. E., & Quinn, P. J. 1989, *MNRAS*, 240, 225
 Villar-Martín, M., Tadhunter, C. N., & Clark, N. 1997, *A&A*, 323, 21
 Villar-Martín, M., Tadhunter, C. N., Morganti, R., Axon, D., & Koekemoer, A. 1999, *MNRAS*, 307, 24

C. Solórzano-Iñarrea and C. N. Tadhunter: Department of Physics and Astronomy, University of Sheffield, Sheffield, S3 7RH, UK (c.solorzano-inarrea,c.tadhunter@sheffield.ac.uk).

D. J. Axon: Department of Physical Sciences, University of Hertfordshire, Hatfield, AL10 9AB, UK (dja@star.herts.ac.uk).